THE JOURNAL OF PHYSICAL CHEMISTRY A

Article

Cite This: J. Phys. Chem. A 2019, 123, 1630−1636

pubs.acs.org/JPCA

Laser Spectroscopy of Methanol Isotopologues in ^{4}He Nanodroplets: Probing the Inertial Response around a Moderately Light Rotor

Isaac Miller,[‡] Ty Faulkner,[‡] and Paul L. Raston*[,†,‡]

[†]Department of Chemistry, University of Adelaide, Adelaide, SA 5005, Australia

[‡]Department of Chemistry and Biochemistry, James Madison University, Harrisonburg, Virginia 22807, United States

ABSTRACT: High-resolution, mid-infrared spectra of methanol isotopologues (CH_3OH, CH_3OD, CD_3OH, and CD_3OD) embedded in superfluid helium nanodroplets have been obtained. For the normal isotopologue, we observed the CO stretching overtone band, the lines within which are 2× broader than in the fundamental for E species methanol and no different than the fundamental for A species methanol. For CH_3OD, we observed the CO stretching overtone band for the first time, which was characterized by narrow line widths for both nuclear spin species. Spectra in the CD_3 stretching bands were much broader, which is attributed to rapid relaxation to nearby anharmonically coupled vibrational state(s). Apparently the coupling is much stronger for CD_3OD, for which the rotational substructure is completely washed out. Inertial analyses of the rotationally resolved fundamental and overtone bands reveal that the moment of inertia of helium, ΔI_{He}, that couples to rotation decreases in going from the heavier (CD_3OH) to lighter (CH_3OH) isotopologues (i.e., with decreasing gas phase moment of inertia, I_G). The dependence of ΔI_{He} on I_G is larger than that found for other molecules in regions approaching the heavy and light rotor limits, which suggests a relatively large breakdown in the adiabatic following of helium density for this moderately light rotor.

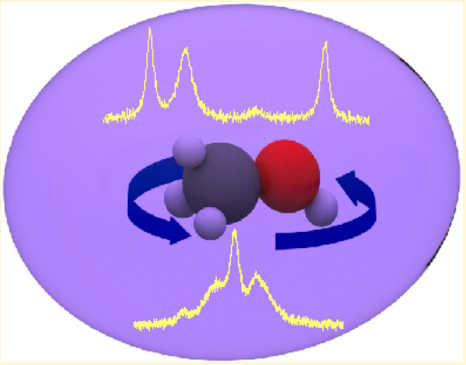

1. INTRODUCTION

High-resolution spectroscopy of molecules embedded in superfluid helium nanodroplets has generated a lot of theoretical interest,[1] ever since the first rotationally resolved spectrum was reported over 20 years ago on SF_6.[2] The rotational constant (inversely proportional to the moment of inertia) was found to be reduced by a factor close to 3 relative to the gas phase, and this was attributed to the coupling of 6−8 helium atoms to molecular rotation. To gain insight, diffusion Monte Carlo calculations were performed that were in agreement with experiment and demonstrated that the degree of coupling between helium and rotor sensitively depends on the rotational constant of the embedded molecule, in addition to the anisotropy of the He-molecule potential;[3] small rotational constants and highly anisotropic potentials favor large couplings (and low effective rotational constants). Furthermore, it was shown that the magnitude of the effective rotational constant is connected with the degree of adiabatic following of helium. When they (fictitiously) reduced the rotational constant of SF_6, a more delocalized helium density distribution was found, implying less helium adiabatically follows molecular rotation. Such "rotational smearing" is often termed the breakdown of the adiabatic following approximation.[4,5]

The first experimental evidence for breakdown of the adiabatic following approximation came from the microwave investigation on HCN and DCN in helium nanodroplets.[6] There, it was found that the moment of inertia of helium, ΔI_{He}, that couples to rotation increases in going from the lighter to heavier isotopologue of "hydrogen" cyanide. Because the helium−molecule potential is the same (to first approximation), the only factor that contributes to the difference is the rotational velocity of the embedded molecule; since HCN rotates faster than DCN, there is more "rotational smearing", implying an increased breakdown in the adiabatic following of helium in the case of HCN. There have been several subsequent studies that have looked at the rotationally resolved spectra of several isotopologues of the same molecule, including (from light to heavy) methane,[7] silane,[7] acetylene,[8] nitrous oxide,[9] and, most recently, carbonyl sulfide.[10] Carbonyl sulfide is the heaviest molecule of the set, for which the degree of adiabatic breakdown was observed to increase as we reduce the moment of inertia of the rotor (in going from ^{18}OCS to ^{16}OCS). This is in line with results from both diffusion Monte Carlo (DMC)[11−13] and reptation quantum Monte Carlo (RQMC),[14] although neither quantitatively accounts for the observed differences between the different isotopologues at this stage.

In an attempt to better understand the relation between adiabatic following and rotational constant, we decided to investigate the isotopologues of methanol, since they fall within an "inertial window" (in-between light and intermediate rotors,

Received: December 31, 2018
Revised: January 29, 2019
Published: February 4, 2019

DOI: 10.1021/acs.jpca.8b12576
J. Phys. Chem. A 2019, 123, 1630−1636

i.e., ∼20−40 amu·Å^2), and cover a broad range of inertias. The normal isotopologue of methanol has previously been investigated in helium nanodroplets, where it was found that the rotational constant is reduced by 56% relative to the gas phase value.[15] Our laser operates around 5 μm, which gives us access to the CD_3 stretch and the CO overtone bands of several methanol isotopologues, as detailed in the following.

2. BACKGROUND

The isotopologues of methanol represent the simplest group of torsional oscillators with C_{3v} symmetry. They have an OX (X = H or D) top that can rotate about the methyl bottom with a 3-fold potential barrier that ranges from 362.12 cm^{-1} (CD_3OD)[16] to 373.5 cm^{-1} (CH_3OH)[17] (note these are empirically determined barriers). Tunneling of the light H/D atoms through the barrier occurs rapidly and results in an appreciable splitting of the torsional states (with quantum number n) into sublevels (with quantum number τ). This splitting amounts to 9.07, 7.12, 2.58, and 1.54 cm^{-1} for the isotopologues of methanol investigated here, i.e., CH_3OH, CD_3OH, CH_3OD, and CD_3OD (see ref 17 and references therein).

Methanol is a prolate top with a very low degree of asymmetry (Ray's asymmetry parameter is 0.98 for CH_3OH), and so for simplicity we treat it as a symmetric top, with rotational quantum numbers J and K for the total rotational angular momentum and its projection onto the principal inertial axis. The CH_3 [CD_3] group contains three identical fermions [bosons], the nuclear spins of which will couple together to give either the A or E nuclear spin symmetry species with a spin degeneracy ratio of 2:1 [11:8].[18] Because two out of three torsional sublevels have E symmetry, and the overall symmetry must satisfy the exclusion principle (i.e., it must have A [i.e., A_1 or A_2 in C_{3v}] symmetry), it follows that the overall population ratio, A:E, for CH_3OX [CD_3OX] is 1:1 [11:16].

In helium nanodroplets, the population of methanol states will mostly collapse down into the ground state, which corresponds (in the ground vibronic state) to J, K, τ = 0, 0, 1 and J, K, τ = 1, 1, 1 for A and E species CX_3OH and to J, K, τ = 0, 0, 1 and J, K, τ = 0, 0, 2 for A and E species CX_3OD (e.g., see Figure 1 in ref 19). All of the bands investigated here have a_1 vibrational symmetry with only an appreciable transition moment along the principal inertial axis. The only relevant selection rules are therefore $\Delta J = \pm 1$ when $K = 0$ and $\Delta J = 0, \pm 1$ when $K = 1$ (for both, $\Delta K = \Delta\tau = 0$).

3. EXPERIMENTAL SECTION

Details of the JMU helium nanodroplet spectrometer have recently been described in detail.[10] It consists of three chambers where droplets are produced, doped, and detected. In brief, we produce helium nanodroplets with an average size of ∼3000 atoms by expanding ultrapure carrier grade (99.9995%) helium at a pressure 40−50 bar through a nozzle (∼5 μm) held at ∼20 K.[20] The middle of the expansion passes through a 0.51 mm (diameter) skimmer and into a second chamber where pickup occurs. We optimized the pressure of methanol for the pickup of either one molecule per droplet (for the CO stretching overtone bands) or ∼0.2 molecules per droplet (CD_3 stretching bands; to minimize cluster formation). Following the pickup of methanol isotopologues, the nanodroplet beam passes through a 5 mm aperture and enters the detection chamber, which houses an off-axis quadrupole mass spectrometer. Helium droplets were ionized by electron impact, and the resulting positively charged fragments were deflected through a quadrupole mass filter, which was set to transmit ions with masses >6 u. An electron multiplier tube detected the ions, and the signal was processed with a dual phase lock-in amplifier that was referenced to the frequency of an "optical" chopper wheel.

The output from a continuous wave quantum cascade laser was split, using a wedged BaF_2 window, into three beams. About 90% of the beam passed through the beamsplitter, which was modulated with the chopper wheel, and directed into the helium nanodroplet machine. The other two beams that were reflected off the front and back of the wedged window were used to determine the wavelength (with a wavemeter) and the relative power (with a thermopile sensor). The depletion signals in this work have been normalized by dividing them by the relative laser power. The laser was tuned using a program developed in LabVIEW,[21] and the data was worked up as described previously.[22] When the laser is resonant with a rotovibrational transition of methanol, absorption can occur, and the excited molecule decays by heating up the droplet which results in evaporation of helium. Because the binding energy of each helium atom is ∼5 cm^{-1},[23] absorption of radiation at 2070 cm^{-1} will (on paper) lead to the loss of ∼400 helium atoms. The spectra reported here correspond to the normalized, inverted ion signal, as a function of wavelength. See refs 24−26 for further details of the technique.

4. OBSERVATIONS AND DISCUSSION

4.1. Spectra and Assignments. *A. Normal Isotopologue (CH_3OH).* Previously, rotovibrational bands around 3 and 10 μm were observed for the normal isotopologue,[15] and here we extend this to 5 μm, wherein lies the CO stretching overtone band. Figure 1 shows a comparison of the spectra in the fundamental and overtone bands and reveals them to be similar, with two differences, relating to the line widths and the A−E splitting. First, the line widths for E species methanol (dotted in Figure 1) are ∼2× broader in the overtone band (∼2 GHz in the overtone versus ∼1 GHz in fundamental) while A species peaks have similar widths (∼0.4 GHz each). The increase in line width with increasing vibrational quantum number is pretty standard in helium nanodroplet spectroscopy (e.g., see ref 27) and results from the increased density of nearby vibrational states (of the correct symmetry) to relax into. The independence of the line width of the A species peaks on the CO stretching state suggests that a similar mechanism is responsible for the line broadening for transitions that access an excited CO stretching state (ν_{CO} = 1 or 2); we suspect this corresponds to a vibration−torsion relaxation pathway. Second, the splitting due to internal rotation of the OH group with respect to the CH_3 group (A−E splitting) increases from 0.296 cm^{-1} in the fundamental to 0.429 cm^{-1} in the overtone band. This is qualitatively consistent with the gas phase, where the analogous splitting increases from 0.475[28] to 0.527 cm^{-1}.[29] We suspect the larger increase in splitting in helium nanodroplets in going from ν' = 1 to 2 relates to different vibration−torsion couplings in comparison to the gas phase. Such a suspicion, however, would require sophisticated calculations to be performed to test (e.g., see ref 30 for "gas phase" calculations).

DOI: 10.1021/acs.jpca.8b12576
J. Phys. Chem. A 2019, 123, 1630−1636

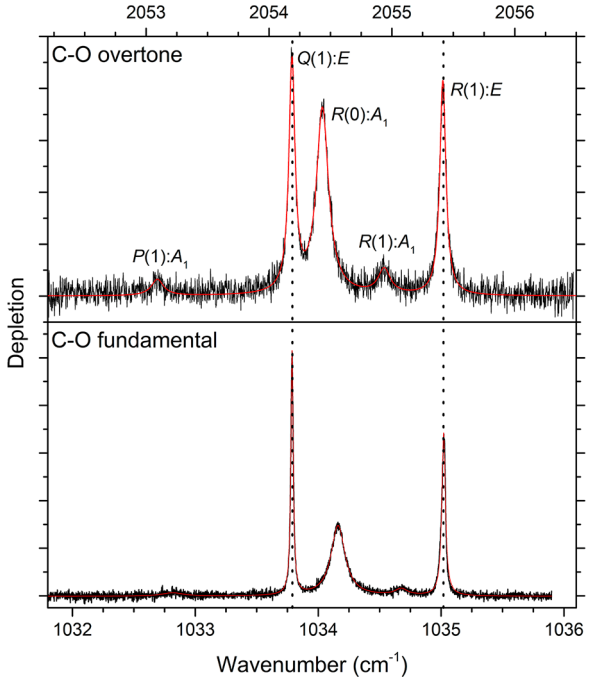

Figure 1. Comparison of the depletion spectra of normal methanol (CH_3OH) in the CO stretching fundamental[15] and overtone bands (pickup chamber pressure [top trace] was ~5 × 10^{-6} Torr). The red curves are simulations using the fitted parameters given in Table 1.

Figure 1 also shows a simulation of the spectrum in the fundamental and overtone bands of methanol using the spectroscopic parameters listed in Table 1. The following nonrigid symmetric top energy level equation was used in the fit, for which we only floated the subband origins [$\nu_{i(A/E)}$] and the excited (vibrational) state rotational constant (B'):

$$\Delta E = \nu_{i(A/E)} + B'_v J'(J'+1) - B''J''(J''+1) - \bar{D}_J[(J'(J'+1))^2 - (J''(J''+1))^2] - \bar{D}_{JK}[(J'(J'+1)) - (J''(J''+1))]K^2$$

The other constants were fixed to those determined in the fit to the fundamental band.[15] The agreement between simulation and experiment is very good, indicating the model we used previously is valid for more highly excited vibrational states.

B. Minor Isotopologues (CH_3OD, CD_3OH, and CD_3OD). Following the observation of the overtone band for the normal isotopologue, we decided to search for the analogous band for CH_3OD. For the normal isotopologue we used the gas phase band origin to guide our spectroscopic search; however, the spectrum for CH_3OD has not been reported in the CO stretching overtone band. To guide our search, we used scaled predictions based on the CO stretching fundamental of CH_3OD, which has been analyzed.[31] We located two peaks that are 0.14 cm^{-1} apart, which correspond to the R(0) transitions of A and E species CH_3OD. This spacing is ~2× the spacing between the subband origins in the corresponding fundamental (i.e., 2 × 0.0654 = 0.131 cm^{-1}).[31] Upon further averaging, we were able to identify transitions from the J'' = 1 states [R(1) and P(1)] as shown in Figure 2. It is hoped that

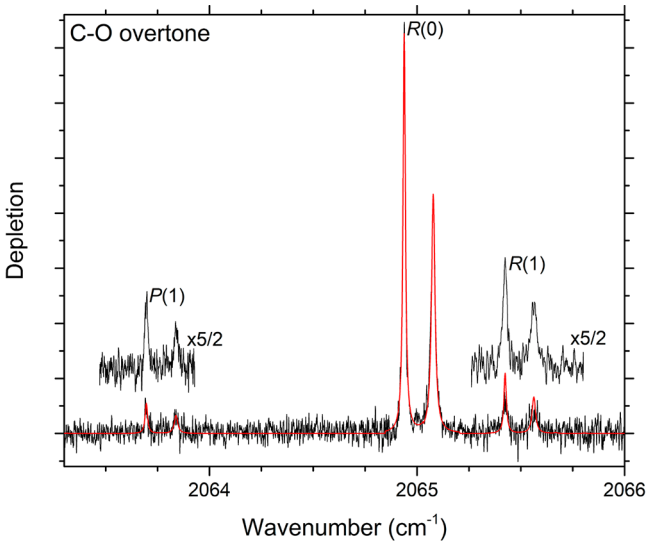

Figure 2. Experimental and simulated infrared spectra of CH_3OD in the CO stretching overtone band (pickup chamber pressure was ~5 × 10^{-6} Torr).

the helium nanodroplet subband origins (see Table 1) could be useful in assigning the gas phase spectrum, which seems reasonable considering that helium nanodroplet band origins are typically within ~2 cm^{-1} of the respective gas phase values.[24] We fit the spectrum using the above equation,

Table 1. Spectroscopic Parameters of Methanol Isotopologues Embedded in Helium Nanodroplets; Uncertainties (in Last place) Are Estimated

constant	CH_3OH[a] C−O fund.	CH_3OH C−O overtone	CH_3OD C−O overtone	CD_3OH C−D_3 fund.	CD_3OD C−D_3 fund.	CH_3OH[a] C−H_3 fund.
B''	0.351(6)	0.351(6)[b]	0.322(5)	0.283(14)[c]		
B'	0.347(6)	0.345(6)	0.319(8)	0.283(14)[c]		
$\bar{D}_J$	0.0063(11)	0.0063(11)[b]	0.0052(9)[d]	0.0042(7)[d]		
$\bar{D}_{JK}$	−0.012(2)	−0.012(2)[b]				
ν_0(A)[e]	1033.498(4)	2053.775(4)	2064.326(10)	2076.06(2)	2074.43(3)[f]	2844.73(2)
ν_0(E)[e]	1033.794(4)	2054.204(4)	2064.468(13)	2076.19(2)	2076.55(2)[f]	2844.96(2)
Γ(A)	0.14(1)	0.12(1)	0.014(2)	0.215(17)	1.1(1)	0.5(1)
Γ(E)	0.029(1)	0.060(2)	0.020(2)	0.594(14)	1.4(1)	0.7(1)
A:E ratio	1:1.01	1:0.98	1:1.03	1:1.9	1:2	1:1.1[g]

[a]From ref 15. [b]Fixed to value determined from fit to fundamental band. [c]Same values assumed for ground and excited states. [d]Estimated by appropriately scaling the relation $D = 0.0310 \times B^{1.818}$.[26] [e]Note that the lowest energy state for the A species is $J_K = 0_0$; for the E species it is 0_0 for CX_3OD (X = H or D) and 1_1 for CX_3OH. [f]Individual lines are not assigned within these two subbands; the values correspond to convoluted peak centers; A/E species assignment should be considered tentative (see main text). [g]Corrected for unassigned R(1) and P(1) line intensity.

DOI: 10.1021/acs.jpca.8b12576
J. Phys. Chem. A 2019, 123, 1630−1636

without the $\bar{D}_{JK}$term, and the resulting simulation using the fitted parameters is shown in Figure 2. It is interesting to note that the line widths are ∼1.4× broader for E species methanol, even though the upper state quantum numbers only differ in τ (which corresponds to the ground state value for each spin isomer).

The CO stretching overtone bands of CD_3OX (X = H or D) are out of range of our laser; however, the relatively strong CD_3 stretching bands are in range. Figures 3 and 4 show

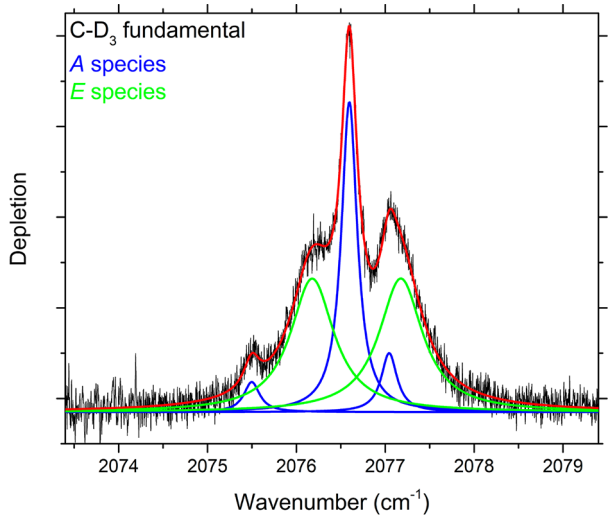

Figure 3. Spectrum of CD_3OH in helium nanodroplets in the symmetric CD_3 stretching fundamental (pickup chamber pressure was 1.0×10^{-6} Torr); for clarity, CD_3OD related peaks have been subtracted (see Figure 4). The blue and green Lorentzian curves correspond to A and E species methanol, respectively, and were fit to the spectrum using the symmetric top equation given in the main text.

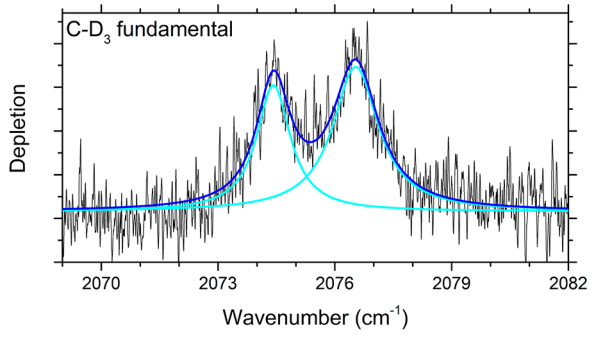

Figure 4. Mid-infrared spectrum of CD_3OD at a very low pickup chamber pressure (7×10^{-7} Torr). The blue curves were generated from a fit of two Lorentzian functions to the data.

spectra in the symmetric CD_3 stretching bands of CD_3OH and CD_3OD, respectively. The line widths are much broader than in the CO stretching bands, which is consistent with what was previously reported for the normal isotopologue.[15] We loosely attribute this to Fermi interactions, which have been predicted to shift the symmetric stretches of CH_3OH, CD_3OH, and CD_3OD by +48.2, +23.6, and +13.6 cm^{-1}, respectively.[32] The shift to higher wavenumber implies there are nearby (lower) vibrational states that the excited state could efficiently couple to in relaxation, thus generally explaining the increased line widths. However, the increase in line widths in going from CD_3OH to CH_3OH to CD_3OD is not proportional to the predicted shifts, as one might expect. Perhaps more involved frequency calculations are required to better predict the shifts, e.g., using the coupled cluster level of theory instead of fourth-order Møller−Plesset theory (that was previously used[32]). Additionally, consideration of interactions other than just Fermi, e.g., Darling−Dennison and Coriolis interactions, that are known to induce intramolecular vibrational energy redistribution,[33] should help uncover the relative importance of line broadening mechanisms for the methanol isotopologues investigated here. Naturally, a full treatment should also consider the interaction with the solvent, which is known to lead to e.g., K-dependent broadening of rovibrational lines of molecules possessing a C_3-axis (e.g., see refs 34 and 35).

For CD_3OH, we partially resolve the rotational substructure, and used the above equation without the $\bar{D}_{JK}$term to fit the spectroscopic parameters to the spectrum (see Table 1 for more details). The simulation shown in Figure 3 matches the measured spectrum well, suggesting the model we used is valid and that the resulting constants are meaningful. Note that there is a large uncertainty for the parameters of CD_3OH because the peaks strongly overlap and thus required deconvolution. In the case of perdeuterated methanol, we fit the spectrum to the sum of two Lorentzian functions (see Figure 4). The resulting relative intensities are 1:2 for the low:high wavenumber peaks, which suggests the assignment should be A:E, based on the closeness to the 1:1.9 ratio for CD_3OH, and qualitative agreement with the expected 1:1.45 ratio based on nuclear spin statistics and torsional degeneracy considerations. We note that for CD_3OD, since we did not resolve individual lines, we cannot be certain of our A:E assignment and that we cannot rule out, e.g., that there is a nearby combination/overtone state that "steals" intensity from the fundamental via a Fermi resonance (which could be the lower wavenumber peak).

4.2. Inertial Analysis. To learn more about the coupling between the solvent and solute, we invert the rotational constant to get the moment of inertia of the complex (i.e., molecule + helium), viz. $I_{He} = \hbar^2/2B$. Then, we determine the moment of inertia of helium (solvent) which couples to the molecule (solute) by $\Delta I_{He} = I_{He} - I_G$, where I_G is the gas phase moment of inertia of the molecule. Figure 5 shows a plot of ΔI_{He} against I_G for the methanol isotopologues we were able to rotationally analyze. Over the small inertial window investigated here (∼5 amu·Å^2), we find a significant variation in ΔI_{He}, in that it increases by ∼7 amu·Å^2. Upon fitting a straight line to the data we see the slope is 1.6, in comparison to 1.0 for OCS,[10] indicating a greater breakdown of the adiabatic following approximation for methanol, which is qualitatively expected since it is a much lighter rotor (in the gas phase, $B_{CH_3OH}/B_{OCS} = 4$).

In ref 7, Hoshina et al. performed an inertial analysis on methane and silane, where they scaled the value of ΔI_{He} for the isotopologues of silane (by 1/4) so that the plot of ΔI_{He} against I_G for both molecules was smooth. Inspired by that we scaled the moments of inertia for several different molecules by a carefully chosen "scaling factor" so that we have a smooth plot. We only included molecules for which a nonrigid rovibrational analysis was performed, the isotopologues were investigated in the same study, and uncertainties in the values of ΔI_{He} were provided. Figure 6 shows the resulting plot, which reveals three different general regions; (III) small I_G values (<10 amu·Å^2) where the gradient is small and converges

DOI: 10.1021/acs.jpca.8b12576
J. Phys. Chem. A 2019, 123, 1630−1636

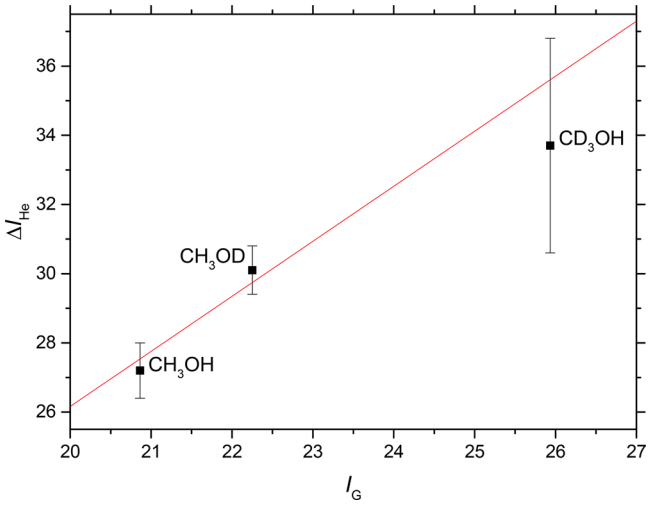

Figure 5. Moment of inertia of helium (ΔI_{He}) plotted against the moment of inertia of the various methanol isotopologues (I_G). Units are amu·Å^2. The red line corresponds to a weighted linear fit (R^2 = 0.83), with a slope of 1.59(48) and an intercept of −5.7(10.4) amu·Å^2.

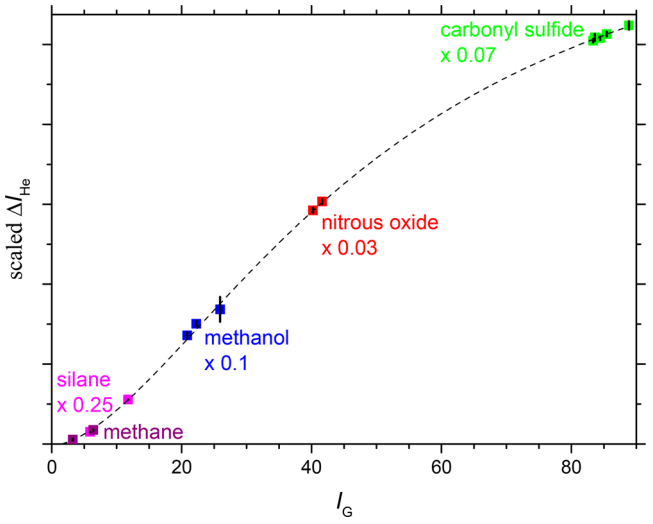

Figure 6. Scaled moment of inertia of helium (scaled ΔI_{He}) plotted against the molecular moment of inertia. In this figure, we only include data from studies that investigated multiple isotopologues of single molecules, for which a centrifugal distortion term was included in the analysis, and uncertainties in the rotational inertias were provided. The scaling factor for each set of isotopologues was chosen so that the plot was smooth; the sigmoidal curve is simply shown to guide the eye.

toward the origin; (II) an intermediate region where the gradient is largest, which includes moderately light to moderately heavy rotors; and (I) large I_G values ($\gtrsim$80 amu·Å^2) where the gradient is small again and seems to be converging toward some limiting value. Note that we label the regions (or regimes) in reverse order to be consistent with the labeling scheme in ref 36.

As discussed previously, the quadratic dependence of ΔI_{He} on I_G in region III suggests that the rotating molecule couples to a vibrating shell of helium atoms (for small I_G values).[7] This picture breaks down as we move into region II, where the coupling evolves into that of a molecule and helium shell that somewhat follows rotation; i.e., there is partial adiabatic following of helium density. In region I we have a molecule coupled to a more rigid helium shell and is converging toward the limit where adiabatic following is complete. Future work should involve investigating a moderately heavy rotor (I_G = 50−70 amu·Å^2) where there is another "inertial gap" and a "massive rotor" for which adiabatic following is basically complete.

We suspect that the values of the scaling factors used in Figure 6 are largely related to the anisotropy of the helium−molecule potential, in addition to the size of the molecule. While we are unable to find sufficiently detailed potentials for SiH_4−He and CH_3OH−He, the anisotropies of the CH_4−He, N_2O−He, and OCS−He potentials have been calculated to be 12,[37] 35,[38] and 21 cm^{-1}.[39] Because a larger anisotropy is known to lead to greater coupling between the molecule and helium, it follows that the largest [smallest] anisotropy qualitatively correlates with the smallest [largest] scaling factors. Deriving a quantitative relationship between the scaling factor and other parameters such as the anisotropy of the helium−molecule potential and size of the molecule would be ideal, but beyond the scope of this work. Rather, we hope the results presented here inspires theoretical investigations along these lines.

5. CONCLUSIONS

We recorded the high-resolution infrared spectra of methanol isotopologues around 4.8−4.9 μm, using a recently built spectrometer. This spectral region allowed for coverage of the CO stretching overtone band of CH_3OH/D and the symmetric CD_3 stretching fundamental of CD_3OH/D. Lines in the CO stretching overtone band were found to be an order of magnitude sharper than those in the stretching fundamental, and we attribute the line broadening to Fermi coupling, which has been theoretically predicted to be important for the symmetric stretch in methanol.[32,40−44] Rovibrational analyses of CH_3OH, CH_3OD, and CD_3OH were possible and allowed for us to fill in an inertial gap that existed in the study of helium solvated isotopologues in the "moderately light rotor" regime. We found that the moment of inertia of helium that couples to rotation increases with that of the methanol isotopologue, according to the relation $\Delta I_{He} \approx 1.6 I_G$, over the small inertial window investigated here (I_G = 21−26 amu·Å^2). This relation puts methanol in the "intermediate region", for which there is a large degree of breakdown of the adiabatic following approximation.

AUTHOR INFORMATION

Corresponding Author

*E-mail: rastonpl@jmu.edu.

ORCID

Paul L. Raston: 0000-0003-3717-4154

Notes

The authors declare no competing financial interest.

ACKNOWLEDGMENTS

Acknowledgment is made to the donors of The American Chemical Society Petroleum Research Fund (56406-UN16) and the National Science Foundation (NSF-REU CHE-1757874).

DOI: 10.1021/acs.jpca.8b12576
J. Phys. Chem. A 2019, 123, 1630−1636

REFERENCES

(1) Szalewicz, K. Interplay Between Theory and Experiment in Investigations of Molecules Embedded in Superfluid Helium Nanodroplets. *Int. Rev. Phys. Chem.* **2008**, *27*, 273−316.

(2) Hartmann, M.; Miller, R. E.; Toennies, J. P.; Vilesov, A. Rotationally Resolved Spectroscopy of SF_6 in Liquid-Helium Clusters - A Molecular Probe of Cluster Temperature. *Phys. Rev. Lett.* **1995**, *75*, 1566−1569.

(3) Lee, E.; Farrelly, D.; Whaley, K. B. Rotational Level Structure of SF_6-Doped ^4He_N Clusters. *Phys. Rev. Lett.* **1999**, *83*, 3812−3815.

(4) Callegari, C.; Conjusteau, A.; Reinhard, I.; Lehmann, K. K.; Scoles, G.; Dalfovo, F. Superfluid Hydrodynamic Model for the Enhanced Moments of Inertia of Molecules in Liquid ^{4}He. *Phys. Rev. Lett.* **1999**, *83*, 5058−5061.

(5) Callegari, C.; Conjusteau, A.; Reinhard, I.; Lehmann, K. K.; Scoles, G.; Dalfovo, F. Erratum: Superfluid Hydrodynamic Model for the Enhanced Moments of Inertia of Molecules in Liquid ^{4}He [Phys. Rev. Lett. 83, 5058 (1999)]. *Phys. Rev. Lett.* **2000**, *84*, 1848−1848.

(6) Conjusteau, A.; Callegari, C.; Reinhard, I.; Lehmann, K. K.; Scoles, G. Microwave Spectra of HCN and DCN in ^{4}He Nanodroplets: A Test of Adiabatic Following. *J. Chem. Phys.* **2000**, *113*, 4840−4843.

(7) Hoshina, H.; Skvortsov, D.; Sartakov, B. G.; Vilesov, A. F. Rotation of Methane and Silane Molecules in He Droplets. *J. Chem. Phys.* **2010**, *132*, 074302.

(8) Nauta, K.; Miller, R. E. The Vibrational and Rotational Dynamics of Acetylene Solvated in Superfluid Helium Nanodroplets. *J. Chem. Phys.* **2001**, *115*, 8384−8392.

(9) Nauta, K.; Miller, R. E. Rotational and Vibrational Dynamics of CO_2 and N_2O in Helium Nanodroplets. *J. Chem. Phys.* **2001**, *115*, 10254−10260.

(10) Faulkner, T.; Miller, I.; Raston, P. L. Quantum Cascade Laser Spectroscopy of OCS Isotopologues in ^{4}He Nanodroplets: A Test of Adiabatic Following for a Heavy Rotor. *J. Chem. Phys.* **2018**, *148*, 044308.

(11) Patel, M. V.; Viel, A.; Paesani, F.; Huang, P.; Whaley, K. B. Effects of Molecular Rotation on Densities in Doped ^{4}He Clusters. *J. Chem. Phys.* **2003**, *118*, 5011−5027.

(12) Viel, A.; Whaley, K. B. Structure and Spectroscopy of Doped Helium Clusters using Quantum Monte Carlo Techniques. *Int. J. Mod. Phys. B* **2003**, *17*, 5267−5277.

(13) Huang, P.; Kwon, Y.; Whaley, K. B. The Finite-Temperature Path Integral Monte Carlo Method and its Application to Superfluid Helium Clusters. In *Microscopic Approaches to Quantum Liquids in Confined Geometries*; World Scientific: 2011; pp 91−128.

(14) Paolini, S.; Fantoni, S.; Moroni, S.; Baroni, S. Computational Spectroscopy of Helium-Solvated Molecules: Effective Inertia, from Small He Clusters Toward the Nanodroplet Regime. *J. Chem. Phys.* **2005**, *123*, 114306.

(15) Raston, P. L.; Douberly, G. E.; Jager, W. Single and Double Resonance Spectroscopy of Methanol Embedded in Superfluid Helium Nanodroplets. *J. Chem. Phys.* **2014**, *141*, 044301.

(16) Müller, H. S. P.; Xu, L.-H.; van der Tak, F. Investigations into the Millimeter and Submillimeter-Wave Spectrum of Perdeuterated Methanol, CD_3OD, in its Ground and First Excited Torsional States. *J. Mol. Struct.* **2006**, *795*, 114−133.

(17) Xu, L. H.; Fisher, J.; Lees, R. M.; Shi, H. Y.; Hougen, J. T.; Pearson, J. C.; Drouin, B. J.; Blake, G. A.; Braakman, R. Torsion-Rotation Global Analysis of the First Three Torsional States (v_t=0, 1, 2) and Terahertz Database for Methanol. *J. Mol. Spectrosc.* **2008**, *251*, 305−313.

(18) The Statistical Weights of the Rotational Levels of Polyatomic Molecules, Including Methane, Ammonia, Benzene, Cyclopropane and Ethylene. *J. Chem. Phys.* **1935**, *3*, 276−285..

(19) Johns, K. P.; Cragg, D. M.; Godfrey, P. D.; Sobolev, A. M. Class II Maser Candidates in Substituted Methanol: CH_3OD, $^{13}CH_3OH$, $CH_3{}^{18}OH$ and CH_3SH. *Mon. Not. R. Astron. Soc.* **1998**, *300*, 999−1005.

(20) Knuth, E.; Schilling, B.; Toennies, J. P. *Proceedings of the 19th International Symposium on Rarefied Gas Dynamics*; Oxford University Press: London, 1995.

(21) Liang, T.; Flynn, S. D.; Morrison, A. M.; Douberly, G. E. Quantum Cascade Laser Spectroscopy and Photoinduced Chemistry of Al-$(CO)_n$ Clusters in Helium Nanodroplets. *J. Phys. Chem. A* **2011**, *115*, 7437−7447.

(22) Morrison, A. M.; Liang, T.; Douberly, G. E. Automation of an "Aculight" Continuous-Wave Optical Parametric Oscillator. *Rev. Sci. Instrum.* **2013**, *84*, 013102.

(23) Pandharipande, V. R.; Zabolitzky, J. G.; Pieper, S. C.; Wiringa, R. B.; Helmbrecht, U. Calculations of Ground-State Properties of Liquid ^{4}He Droplets. *Phys. Rev. Lett.* **1983**, *50*, 1676−1679.

(24) Toennies, J. P.; Vilesov, A. F. Superfluid Helium Droplets: A Uniquely Cold Nanomatrix for Molecules and Molecular Complexes. *Angew. Chem., Int. Ed.* **2004**, *43*, 2622−2648.

(25) Stienkemeier, F.; Lehmann, K. K. Spectroscopy and Dynamics in Helium Nanodroplets. *J. Phys. B: At., Mol. Opt. Phys.* **2006**, *39*, R127−R166.

(26) Choi, M. Y.; Douberly, G. E.; Falconer, T. M.; Lewis, W. K.; Lindsay, C. M.; Merritt, J. M.; Stiles, P. L.; Miller, R. E. Infrared Spectroscopy of Helium Nanodroplets: Novel Methods for Physics and Chemistry. *Int. Rev. Phys. Chem.* **2006**, *25*, 15−75.

(27) Callegari, C.; Conjusteau, A.; Reinhard, I.; Lehmann, K. K.; Scoles, G. First Overtone Helium Nanodroplet Isolation Spectroscopy of Molecules Bearing the Acetylenic CH Chromophore. *J. Chem. Phys.* **2000**, *113*, 10535−10550.

(28) Villanueva, G. L.; DiSanti, M. A.; Mumma, M. J.; Xu, L. H. A Quantum Band Model of the ν_3 Fundamental of Methanol (CH_3OH) and its Application to Fluorescence Spectra of Comets. *Astrophys. J.* **2012**, *747*, 37.

(29) High-resolution spectrum of the C-O stretch overtone band in methyl alcohol. *J. Chem. Phys.* **1990**, *93*, 7049−7053..

(30) Perry, D. S. The Adiabatic Approximation as a Diagnostic Tool for Torsion-Vibration Dynamics. *J. Mol. Spectrosc.* **2009**, *257*, 1−10.

(31) Lundsgaard, A.; Petersen, J. C.; Henningsen, J. High-Resolution Fourier-Transform Spectrum of the C-O Stretch Band of CH_3OD. *J. Mol. Spectrosc.* **1994**, *167*, 131−155.

(32) Miani, A.; Hanninen, V.; Horn, M.; Halonen, L. Anharmonic Force Field for Methanol. *Mol. Phys.* **2000**, *98*, 1737−1748.

(33) Lehmann, K. K.; Scoles, G.; Pate, B. H. Intramolecular Dynamics from Eigenstate-Resolved Infrared-Spectra. *Annu. Rev. Phys. Chem.* **1994**, *45*, 241−274.

(34) Morrison, A. M.; Raston, P. L.; Douberly, G. E. Rotational Dynamics of the Methyl Radical in Superfluid ^{4}He Nanodroplets. *J. Phys. Chem. A* **2013**, *117*, 11640.

(35) Lemeshko, M. Quasiparticle Approach to Molecules Interacting with Quantum Solvents. *Phys. Rev. Lett.* **2017**, *118*, 095301.

(36) Suárez, A. G.; Ramilowski, J. A.; Benito, R. M.; Farrelly, D. Renormalization of the Rotational Constants of an Ammonia Molecule Seeded into a ^{4}He Droplet. *Chem. Phys. Lett.* **2011**, *502*, 14−22.

(37) Calderoni, G.; Cargnoni, F.; Martinazzo, R.; Raimondi, M. Potential Energy Surface, Bound States, and Rotational Inelastic Cross Sections of the He-CH_4 System: A Theoretical Investigation. *J. Chem. Phys.* **2004**, *121*, 8261−8270.

(38) Chang, B. T.; Akin-Ojo, O.; Bukowski, R.; Szalewicz, K. Potential Energy Surface and Rovibrational Spectrum of He−N_2O Dimer. *J. Chem. Phys.* **2003**, *119*, 11654−11670.

(39) Howson, J. M.; Hutson, J. M. Morphing the He−OCS Intermolecular Potential. *J. Chem. Phys.* **2001**, *115*, 5059−5065.

(40) Halonen, L. Theoretical Study of Vibrational Overtone Spectroscopy and Dynamics of Methanol. *J. Chem. Phys.* **1997**, *106*, 7931−7945.

(41) Hanninen, V.; Horn, M.; Halonen, L. Torsional Motion and Vibrational Overtone Spectroscopy of Methanol. *J. Chem. Phys.* **1999**, *111*, 3018−3026.

DOI: 10.1021/acs.jpca.8b12576
J. Phys. Chem. A 2019, 123, 1630−1636

(42) Hanninen, V.; Halonen, L. Calculation of Spectroscopic Parameters and Vibrational Overtones of Methanol. *Mol. Phys.* **2003**, *101*, 2907−2916.
(43) Sibert, E. L.; Castillo-Chara, J. Theoretical Studies of the Potential Surface and Vibrational Spectroscopy of CH_3OH and its Deuterated Analogs. *J. Chem. Phys.* **2005**, *122*, 194306.
(44) Perchard, J. P.; Romain, F.; Bouteiller, Y. Determination of Vibrational Parameters of Methanol from Matrix-Isolation Infrared Spectroscopy and *Ab Initio* Calculations. Part 1 - Spectral Analysis in the Domain 11000−200 cm^{-1}. *Chem. Phys.* **2008**, *343*, 35−46.

DOI: 10.1021/acs.jpca.8b12576
J. Phys. Chem. A 2019, 123, 1630−1636